UCRL-JC-124865
PREPRINT

High Fluence 1.05 μm Performance Tests using 20 ns Shaped Pulses on the Beamlet Prototype Laser

B. Van Wonterghem, J. E. Murray, S. C. Burkhart,
F. Penko, M. A. Henesian, J. A. Auerbach,
P. J. Wegner, and J. A. Caird

This paper was prepared for submittal to the
2nd Annual International Conference on Solid-State
Lasers for Application to Inertial Confinement Fusion
Paris, France
October 22-25, 1996

December 27, 1996

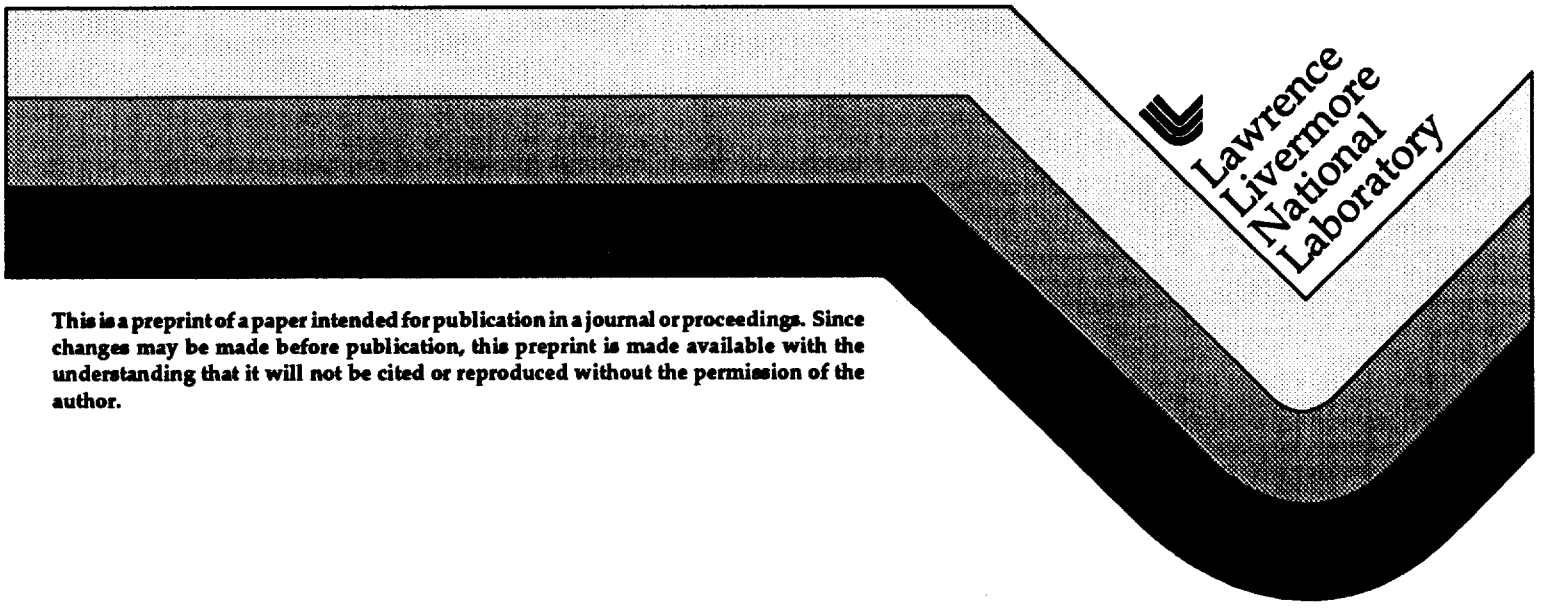

High Fluence 1.05 μm **performance tests using 20 ns shaped pulses on the Beamlet prototype laser**[†]

B. M. Van Wonterghem, J.E. Murray, S.C. Burkhart, F. Penko, M.A. Henesian, J.A. Auerbach, P.J. Wegner and J.A. Caird

Lawrence Livermore National Laboratory
P.O. Box 808, Livermore, CA 94550

ABSTRACT

Beamlet is a single beamline, nearly full scale physics prototype of the 192 beam Nd:Glass laser driver of the National Ignition Facility. It is used to demonstrate laser performance of the NIF multipass amplifier architecture. Initial system characterization tests have all been performed at pulse durations less than 10 ns. Pinhole closure and modulation at the end of long pulses are a significant concern for the operation of NIF. We recently demonstrated the generation, amplification and propagation of high energy pulses temporally shaped to mimic 20 ns long ignition pulse shapes at fluence levels exceeding the nominal NIF design requirements for Inertial Confinement Fusion by Indirect Drive. We also demonstrated the effectiveness of a new conical pinhole design used in the transport spatial filter to mitigate plasma closure effects and increase closure time to exceed the duration of the 20 ns long pulse. **Keywords**: inertial confinement fusion, Nd:glass lasers, spatial filter

1. INTRODUCTION

The Beamlet laser is a single-aperture Nd:Glass laser system that functions as a scientific prototype of a new class of fusion laser drivers. Its architecture is based on the use of components with a single aperture size. The beam propagates multiple passes through the largest aperture amplifier, rather than through a series of increasing aperture amplifiers. Initial passes at low fluence use the full gain of the full aperture amplifiers without extracting significant energy, thereby replacing costly preamplifier stages. Multipass amplification is achieved by building an image relayed cavity around the main amplifiers. This type of architecture proves to be cost effective and most suitable to stack amplifier chains into compact powerful arrays, designed to deliver the required energy on target after frequency conversion of the 1.05 μm beam to 0.351 μm. The National Ignition Facility is designed to deliver 1.8 MJ of 0.351 nm light at the entrance of an Indirect Drive Hohlraum target. It uses 192 beams arranged in 24 bundles of 8 beamlines [1-3]. The multi-segment amplifiers are 4 slabs high by 2 slabs wide. The NIF driver however provides

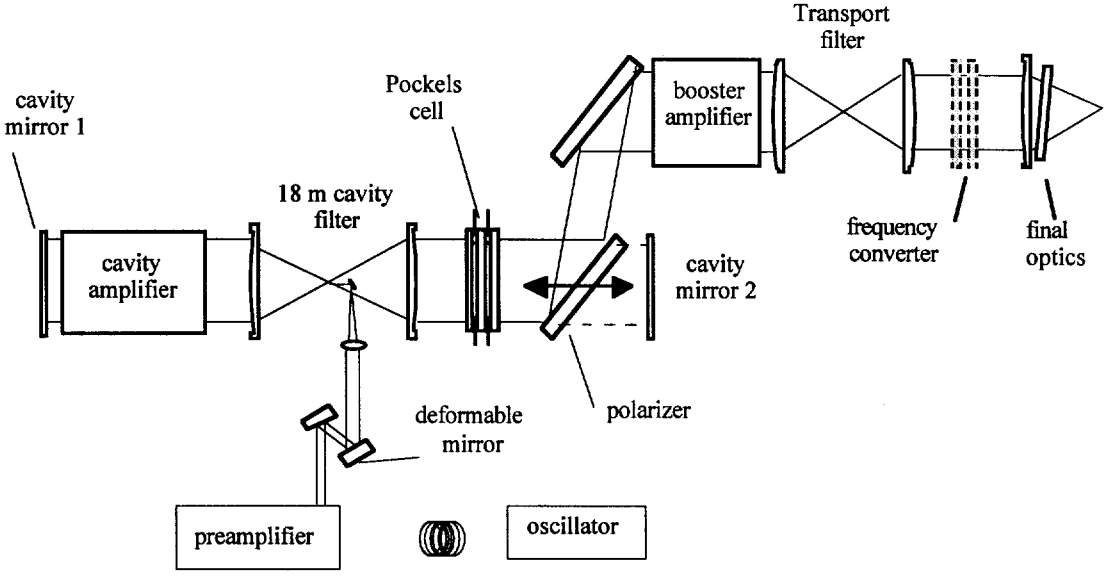

Figure 1. Schematic lay out of the Beamlet multipass Nd:glass laser

[†] This work was performed under the auspcies of the U.S. Department of Energy by the Lawrence Livermore National Laboratory under contract No. W-7405-Eng-48.

performance over a wide range of pulse durations to accommodate various types of user experiments.

The actual Beamlet lay-out as shown in figure 1 is very close to the NIF driver design[4]. The laser consists of a preamplifier, and two large amplifier stages: a four-pass cavity amplifier, and a single pass booster amplifier. The cavity amplifier uses 11 Brewster angled slabs in a 36 meter long image relayed cavity, which is build up using two end mirrors, a spatial filter relay telescope, and an optical switch consisting of a large aperture polarizer and Plasma Electrode Pockels cell (PEPC). Beamlet uses multi-segment amplifiers two slabs wide by two slabs high. Only one of the apertures however is equipped with laser glass. The pulse is injected near the focal plane of the cavity spatial filter using a small injection mirror. The beam is allowed to make four passes through the cavity amplifier with the optical switch turned on, and is then reflected from the cavity polarizer. The five slab long booster amplifier provides additional amplification and delivers typically 12 kJ in 3 ns, the Beamlet design point. The beam is then spatially filtered and relayed to the location of the frequency converter. A large set of diagnostic systems is used to analyze the 1.05 μm and the 351 nm beams. The long pulse experiments in this paper were limited to 1.05 μm and the frequency converter crystals were replaced by a beam dump. Frequency conversion of high fluence, long pulses will be tested with a NIF prototype final optics configuration that is being designed and constructed at this time.

The experiments described in this paper investigate the performance of the Beamlet prototype under conditions close to Indirect Drive ICF requirements. The pulse shape consists of a long low intensity foot, approximately 17 ns long, and a 3-4 ns high intensity main part. The main issues addressed during these experiments is the generation and amplification of these long pulses, and a first evaluation of pinhole closure effects in the spatial filters, configured for a spatial cutoff frequency of ±200 μrad. This corresponds to a diameter of 3.6 mm for the 18 meter long Beamlet cavity and transport spatial filters. As will be discussed later, the Beamlet transport spatial filter is approximately three times shorter than the NIF transport filter and consequently a three times smaller F#. The Beamlet experiments are therefore much more stringent than the NIF conditions for the transport spatial filter, but are actually close to simulating the NIF cavity spatial filter.

2. APPLICATION OF NEW PULSE SHAPING TECHNIQUES ON BEAMLET

Pulse shaping is accomplished on Beamlet using low voltage waveguide type electro-optic modulation techniques in integrated optical circuits. This new system also presents the basis for the NIF pulse shaping system and has been described previously [5]. A hybrid electronic scheme was used to generate a long, low intensity foot with 20.5 ns pulse length, while a second Arbitrary Waveform Generator was used to create the complex main pulse with a total length of 7 ns [6]. Using this system, we could create as well long square output pulses, as pulses with

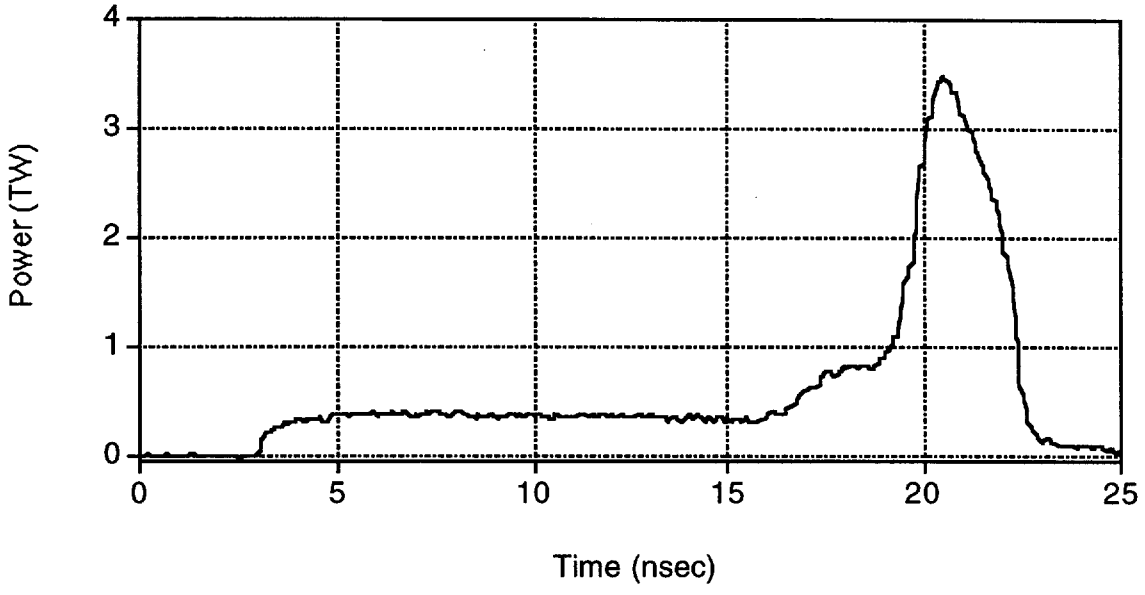

Figure 2. Power of the 1.05 μm output beam on a typical long pulseshot. The input power contrast required to generate this pulse shape was 80:1.

an ignition like shape. During the course of this experiment, pulses with a complex shape and very large dynamic range (up to 100:1) were successfully generated. Figure 2 shows a typical 1.05 μm temporal power trace for pulses used during these experiments. Typically the desired 1.05 μm contrast (peak power to foot power ratio) at the output of the amplifiers is 10:1 for Indirect Drive conditions. The actual contrast of the 351 nm pulses is increased by the power dependence of the frequency conversion process.

3. PERFORMANCE LIMITS OF THE LASER USING LONG, SHAPED PULSES

Large Nd:glass lasers, such as Beamlet, have a number of design parameters that can be altered to optimize the energy/intensity performance for a particular pulse length and shape. The limitations to this optimization are stored energy in the laser slabs, the optical damage threshold of the individual components, and the nonlinear growth of the beam modulation (B-integral effect). Beamlet was designed to provide optimum performance for a temporally square 3 ns output pulse. At this operating point both B-integral in the cavity and the booster section are at a set limit, and the fluence of the cavity polarizer is at nearly 70 % of its safe operating fluence limit (11 J/cm^2, 3 ns pulse).

Figure 3 shows a calculated safe NIF operating curve for square output pulses plotted in intensity versus fluence space, data points from over. 500 Beamlet shots using square temporal pulses, and a new set of results obtained with 20 ns shaped output pulses. Beamlet runs with a square aperture that can be varied from 30 to 35 cm edge size and effective area between 740 and 1100 cm^2. All Beamlet energy and power data on figure 3 were scaled to the NIF beam area of 1260 cm^2. The calculation is based on either a nonlinear phase shift between spatial filters, ΔB, equal to 1.8 radians, damage threshold of optical components, and extraction limit of the amplifier chain. Shots of equal pulse duration are located on lines though the origin. At low output energies, ΔB in the booster amplifier

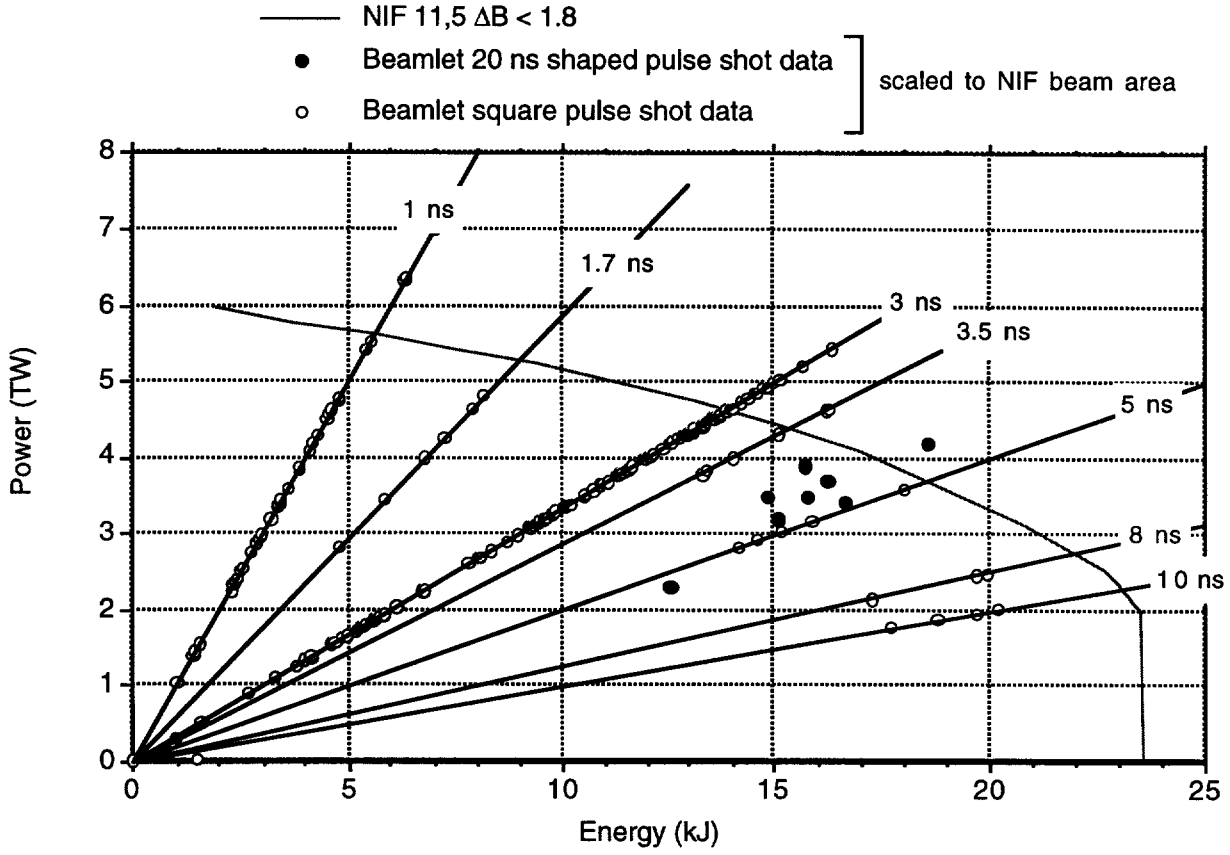

Figure 3. NIF 11-5 amplifier configuration safe performance limit with scaled Beamlet experimental data points, including recent long pulse shots.

section is the limiting factor. As the fluence (and pulse duration increases), the input power needs to be temporally shaped to compensate for gain saturation, leading to lower intensity limits. When the gain in the booster amplifier

is largely saturated, and saturation increases in the cavity amplifiers, the ΔB in the cavity rises sharply and becomes the limiting factor. At even longer pulse durations, the stored energy limits the performance and the sharp drop in the performance indicates the extraction limit. Long shaped pulses are characterized by an equivalent pulse duration (EPD), which is defined as the ratio of energy over peak power. EPD for 1.05 μm shots is between 4 and 5 ns, at the output of the laser. The EPD changes during amplification as a consequence of saturation, and is approximately 3.5 ns at the exit of the cavity amplifier. EPD is important since it used in the calculation of damage thresholds for optical components in the amplifier chain.

Experimentally, performance and beam quality are evaluated based on near field and far field diagnostics to characterize near field modulation and far field spot size. Near field modulation is characterized by the contrast ratio, defined as average normalized RMS intensity fluctuation over the beam's area. Nonlinear modulation growth depends on ΔB, and for a shaped output pulse, reaches a peak during a specific time slice of the pulse. The imaging diagnostics as discussed above are inadequate to evaluate this noise growth and the ΔB-limits of the laser for long pulses. An extensive experimental campaign and theoretical analysis was launched to investigate these conditions using short 200 ps pulses propagated under conditions simulating the worst case for noise growth, and is described elsewhere Widmayer et al.[7]. The results demonstrate that by limiting high angle scattering through appropriate spatial filtering of the beams, and by using components with low surface roughness, on the order of 10 Å RMS measured over scale lengths of 33 to 0.12 mm, high quality beams can be obtained under operating conditions consistent with NIF red-line performance requirements.

4. PINHOLE CLOSURE LIMITATIONS

One of the main issues related to the propagation and amplification of long pulses is pinhole closure in the spatial filters of the laser chain. It is well known that high angle scattered light irradiates the edge of the pinhole in the focal plane of the spatial filters, and creates a low density plasma that subsequently propagates into the pinhole aperture. After some time, the density within the pinhole can reach a level where it will affect the quality of the propagating beam, even long before opacity of the plasma becomes a problem. Phase gradients as a consequence of plasma density gradients scatter light within the clear aperture of the output lens of the spatial filter and cause a redistribution of the energy in the near field.

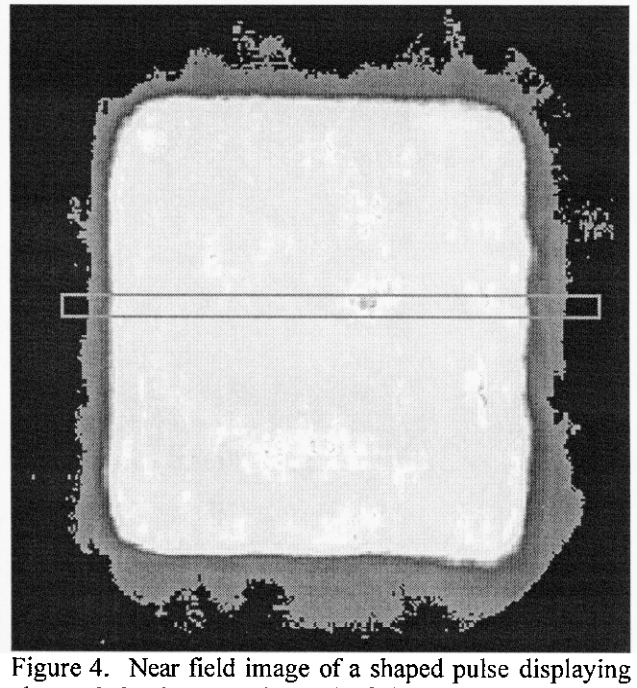

Figure 4. Near field image of a shaped pulse displaying closure behavior near the end of the pulse. The framed area corresponds to the segment that is imaged on a streak camera slit for time resolved analysis.

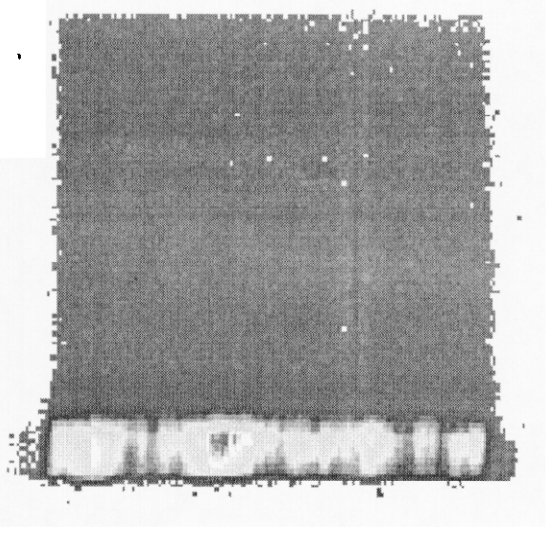

Figure 5. Streaked near field segment corresponding to a small segment of the near field image shown in figure 4, Time runs from top to bottom. The total pulse length is 20.5 ns. Modulation grows quickly after 17 ns.

Closure speed depends on the details of the pinhole design and material, and the edge irradiation, which is determined by the pinhole size, spatial filter F#, and the intensity in the pulse[8]. Typically, Beamlet operates with ±200 μrad pinholes (3.6 mm diameter), made from high density graphite carbon. Pinhole closure was observed with these 'washer' geometry pinholes when the pulse power exceeded 0.4 TW in a 34.5 cm beam (effective beam area 1050 cm^2). The near field image shows the energy scattered outside the beam's edge. Figure 4 shows a near field of a shaped pulse, where closure has affected beam modulation during the last 3.5 ns of the pulse, i.e. the time slice that contains the main pulse, and therefore a large fracture of the total energy. Closure is indicated clearly in a time resolved near field segment shown in figure 5. The bottom part of the streak is the main pulse which displays a long spatial frequency modulation with peak-to-average modulation exceeding 2:1. Calorimetry measurements indicate an energy loss of 200 J, nearly 1.5 % of the total energy in the pulse.

Experiments with 20 ns temporally square pulses and similar pinholes indicate that the closure is independent of the presence of the main pulse. Figure 6 shows the time resolved near field modulation reduced from the streaked near field segments for two levels of power in the foot of a shaped pulse, and a temporally square pulse.

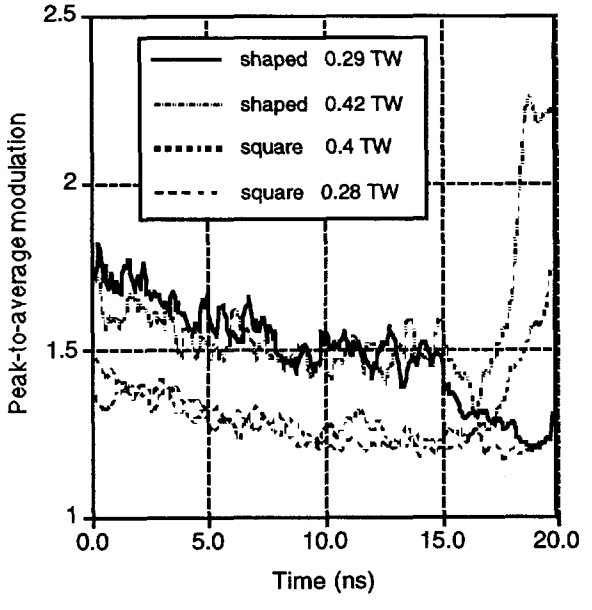

Figure 6. Time resolved peak-to-average-near field modulation during a 20 ns pulse extracted from streaked near field data. The sudden rise in the modulation near the end of the pulse is a signature of pinhole closure effects.

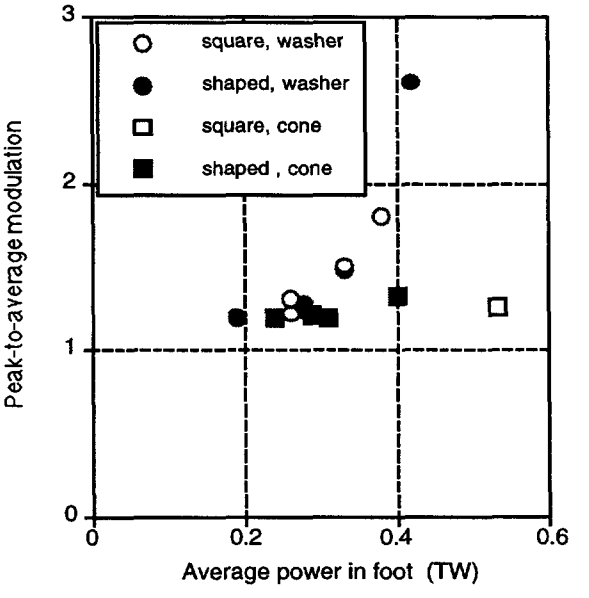

Figure 7. Peak-to-average near field modulation at 20 ns as function of foot power for two different pinholes. Results are shown for pulses with and without a main pulse present.

Shaped pulses had a nominally 10: 1 contrast at the output of the laser. The initial drop in spatial modulation is caused by the gain saturation in the amplifiers. Pulses with foot power of 0.3 TW do not show a rising modulation as shown by the pulses with foot power above 0.4 TW. The modulation rises after about 17 ns, and indicates a closure speed of nearly 10^7 cm/s. At 0.4 TW, the azimuthally averaged edge irradiance on the pinhole is estimated at 4.10^9 W/cm^2 based on Schlieren far field images. The peak edge irradiance at 200 μrad is located on the axes of the diamond shaped far field pattern and is about an order of magnitude higher. Even when closure was observed on the forward propagating beam through the transport spatial filter, no backreflections were observed on the backscatter diagnostic in the injection beamline.

Subsequent experiments used a new pinhole design to replace the carbon washer pinhole in the transport spatial filter. This pinhole had a long conical entrance to reduce the absorption on the edge of the entrance aperture, and deflect unwanted rays outside the laser's clear aperture with a reduced absorption on the pinhole walls. The cone aperture angle is matched to the spatial filter f# and its length is chosen such that the cone aperture is nearly two times wider than the effective filtering aperture at the end of the cone. Off-line results indicated a significant increase in closure time with this design[8]. Figure 7 compares the time-reolved near field modulation at the end of the pulse using a conical stainless steel pinhole, and a carbon washer pinhole. Figure 8 shows a picture of three different

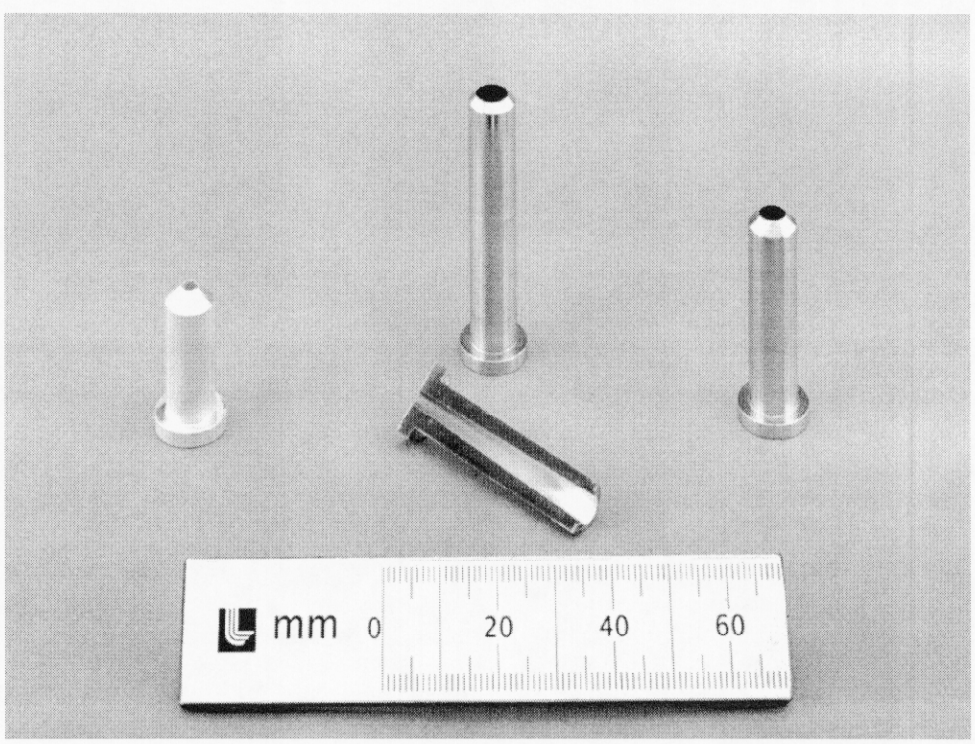

Figure 8. Photograph of the conical pinholes that were used to replace the carbon washer pinholes. The cut pinhole in the foreground shows the conical aperture. No closure effects were observed with the ±200 μr conical pinhole at foot intensities exceeding 0.5 TW.

conical pinholes designed for use on Beamlet. Further experiments will isolate the influence of the pinhole material itself on closure speed.

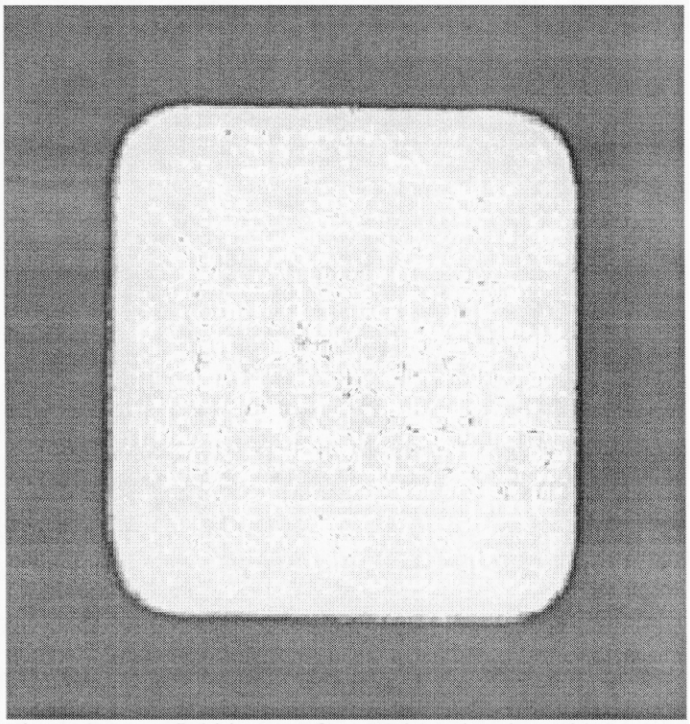

Figure 9. Near field image of a 15.3 kJ pulse shot with 20.5 ns ignition pulse shape at 1.05 μm.

The foot power under the nominal NIF 1.8 MJ 351 nm indirect drive condition is 0.35 TW in the corresponding 1.05 μm beams. This power is close to the closure threshold observed in the carbon washer pinhole shots. Scaling the Beamlet results to a NIF like spatial filter F# requires detailed knowledge of the scaling laws of closure with respect to pinhole size and material (Z number). The NIF spatial filter is nearly 3 times longer than the Beamlet spatial filter, using 9 m focal length lenses compared to 30 m in the NIF design. This increases as well the pinhole size corresponding to a ±200 μr cut-off angle, as the edge irradiance itself. Detailed verification of the plasma physics model and calculations using LASNEX are being performed using these results and off-line experiments. This effort is discussed in more detail elsewhere in these proceedings[9]. Further experiments will also evaluate spatial filtering down to the desired spatial filtering for NIF, which is ±100 μrad rather than the ±200 μrad filtering used in these experiments. The ± 100 μrad cutoff is required to maintain the necessary safety margin against small scale self-focusing under NIF operating conditions.

5. BEAMLET 1.05 μm PERFORMANCE RESULT NEAR NIF INDIRECT DRIVE CONDITIONS

Beam performance was evaluated using an extensive set of 1.05 μm diagnostics. This includes evaluation of near field modulation with high resolution near field cameras, far field spot size and small angle scatter outside ±33 μrad using a time resolved Schlieren technique. Figure 9 shows the near field of the highest energy shaped pulse shot (15.3 kJ). The following list summarizes the main performance results for this shot:

Output energy	15.3 kJ
Average fluence	14.7 J/cm^2
Peak fluence	20.5 J/cm^2
Equivalent pulse duration	4.45 ns
Peak power	3.4 TW
Near field modulation	1.33:1
Near field contrast	0.09
80% spot radius	15.6 μrad
Fraction outside ±33 μrad	0.033
Hartmann sensor wavefront	1.1 λ pk-valley, 0.22 λ RMS.

Detailed analysis and modeling of these preliminary results is in progress and will be published elsewhere.

6. CONCLUSIONS

We have tested operation of the Beamlet prototype laser at 1.05 μm under conditions equivalent to NIF indirect drive requirements. A hybrid pulse shaping system created a 20.5 ns shaped pulses with a 17 ns foot and 3 ns main pulse. Pinhole closure was observed using ±200 μrad carbon pinholes, but was absent when replaced by a newly designed conical pinhole. Future Beamlet campaigns will address closure with tighter ±100 μrad pinholes and frequency conversion using a NIF like final optics prototype assembly.

7. REFERENCES

1. National Ignition Facility Conceptual Design Report, UCRL-PROP-117093 (May 1994). Available from the National Technical Information Service, US Dept of Commerce, 5285 Port Royal Rd, Springfield, VA 22161.
2. W.H. Lowdermilk, "Status of the National Ignition Facility project", these proceedings.
3. John Lindl, " Development of the Indirect Drive approach to inertial confinement fusion and the target physics basis for ignition and gain," Phys. of Plasmas, 2, 3933 (1995)
4. B.M. Van Wonterghem, J.R. Murray, J.H. Campbell, D.R. Speck, C.E. Barker, I.C. Smith, D.F. Browning and W.C. Beherendt, "Performance of a prototype, large-aperture multipass ND-glass laser for Inertial Confinement Fusion", accepted for publication in Applied Optics.
5. R.W. Wilcox and D.F. Browning, ICF Quarterly Report 2(3), 115-122, Lawrence Livermore National Laboratory, CA, UCRL-LR-105821-92-3 (1992)
6. S.C. Burkhart, R. Wilcox, F. Penko, D. Browning, "Amplitude and phase modulation with waveguide optics", these proceedings.
7. C.C. Widmayer, J.M. Auerbach, R.B Ehrlich, M.A. Henesian, J.T. Hunt e.a., "Producing National Ignition Facility (NIF) - quality beams on the Nova and Beamlet lasers", to be published in Proceeedings of the 12th ANS Topical Meeting on the Technology for Fusion Energy, Reno, NV, June 7-13, 1996.
8. P. Celliers, K. Estabrook, R.J. Wallace, J.E. Murray, L.B. Da Silva, B.J. MacGowan, B.M. Van Wonterghem, J.T. Hunt K. Manes,"A novel spatial filter pinhole for high energy pulsed lasers", 24th European Conference on Laser Interaction with Matter, Madrid, Spain, 3-7 June 1996.
9. J.E. Murray, K.G. Estabrook, D. Milam, W.D. Sell, B. M. Van Wonterghem, M.D. Feit, A.M. Rubenchik, "Spatial Filter Issues", these proceedings.

Technical Information Department • **Lawrence Livermore National Laboratory**
University of California • Livermore, California 94551